

Resonant coupling from a new angle: coherent control through geometry

N. Rotenberg,^{1,*} D. M. Beggs,¹ J. E. Sipe² and L. Kuipers¹

¹Center for Nanophotonics, FOM Institute AMOLF, Science Park 104, 1098 XG, Amsterdam, The Netherlands

²Department of Physics and Institute for Optical Sciences, University of Toronto, Toronto, Ontario, M5S 1A7, Canada

* rotenberg@amolf.nl

Abstract: We demonstrate that interference of absorption pathways can be used to control resonant coupling of light to guided modes in a manner analogous to quantum coherent control or electronically induced transparency. We illustrate the control of resonant coupling that interference affords using a plasmonic test system where tuning the phase of a grating is sufficient to vary the transfer of energy into the surface plasmon polariton by a factor of over 10^6 . We show that such a structure could function as a one-way coupler, and present a simple explanation for the underlying physics.

© 2013 Optical Society of America

OCIS codes: (240.6690) Surface waves; (260.5740) Resonance; (050.1960) Diffraction theory.

References and links

1. J. M. Fraser, A. I. Shkrebti, J. E. Sipe, and H. M. van Driel, "Quantum interference in electron-hole generation in noncentrosymmetric semiconductors," *Phys. Rev. Lett.* **83**, 4192-4195 (1999).
2. S. E. Harris, "Electromagnetically induced transparency," *Phys. Today* **50**, 36-42 (1997).
3. W. Wan, Y. Chong, L. Ge, H. Noh, A. Douglas Stone, and H. Cao, "Time-reversed lasing and interferometric control of absorption," *Science* **311**, 889-892 (2011).
4. B. Luk'yanchuk, N. I. Zheludev, S. A. Maier, N. J. Halas, P. Norlander, H. Giessen, and C. T. Chong, "The Fano resonance in plasmonic nanostructures and metamaterials," *Nat. Materials* **9**, 707-715 (2010).
5. M. Born and E. Wolf, *Principles of Optics* (Cambridge University Press, 1999).
6. L. Liu, R. Kumar, K. Huybrechts, T. Spuesens, G. Roelkens, E.-J. Geluk, T. de Vries, P. Regreny, D. Van Thourhout, R. Baets, and G. Morthier, "An ultra-small, low-power, all-optical flip-flop memory on a silicon chip," *Nature Photon.* **4**, 182-187 (2010).
7. H. Raether, *Surface Plasmons*, edited by G. Hohler (Springer, Berlin, 1988).
8. N. Rotenberg and J. E. Sipe, "Analytic model of plasmonic coupling: Surface relief gratings," *Phys. Rev. B* **83**, 045416 (2011).
9. J. Chandezon, M. T. Dupuis, G. Cornet, and D. J. Maystre, "Multicoated gratings: a differential formalism applicable in the entire optical region," *Opt. Soc. Am.* **72**, 839-846 (1982).
10. L. Li, J. Chandezon, G. Granet, and J.-P. Plumey, "Rigorous and efficient grating-analysis method made easy for optical engineers," *Appl. Opt.* **38**, 304-313 (1999).
11. M. G. Moharam, E. B. Grann, D. A. Pommet, and T. K. Gaylord, "Formulation for stable and efficient implementation of the rigorous coupled-wave analysis of binary gratings," *J. Opt. Soc. Am. A* **12**, 1068-1076 (1995).
12. M. G. Moharam, E. B. Grann, D. A. Pommet, and T. K. Gaylord, "Stable implementation of the rigorous coupled-wave analysis for surface-relief gratings: enhanced transmittance matrix approach," *J. Opt. Soc. Am. A* **12**, 1077-1086 (1995).
13. S. Fan, R. Baets, A. Petrov, Z. Yu, J. D. Joannopoulos, W. Freude, A. Melloni, M. Popović, M. Vanwolleghem, D. Jalas, M. Eich, M. Krause, H. Renner, E. Brinkmeyer, and C. R. Doerr, "Comment on Nonreciprocal light propagation in a silicon photonic circuit," *Science* **335**, 38 (2012).
14. M. C. Hutley, *Diffraction Gratings* (Academic Press, New York, 1982).

15. N. Bonod, E. Popov, L. Li, and B. Chernov, "Unidirectional excitation of surface plasmons by slanted gratings," *Opt. Express* **15**, 11427-11432 (2007).
16. W. L. Barnes, T. W. Preist, S. C. Kitson, and J. R. Sambles, "Physical origin of photonic energy gaps in the propagation of surface plasmons on gratings," *Phys. Rev. B* **54**, 6227-6244 (1996).
17. R. A. Watts, A. P. Hibbins, and J. R. Sambles, "The influence of grating profile on surface plasmon polariton resonances recorded in different diffracted orders," *J. Mod. Opt.* **46**, 2157-2186 (1999).
18. G. Maisons, M. Carras, M. Garcia, O. Parillaud, B. Simozrag, X. Marcadet, and A. De Rossi, "Substrate emitting index coupled quantum cascade lasers using biperiodic top metal gratings," *Appl. Phys. Lett.* **94**, 151104 (2009).
19. I. Dolev, M. Volodarsky, G. Porat, and A. Arie, "Multiple coupling of surface plasmons in quasiperiodic gratings," *Opt. Lett.* **36**, 1584-1586 (2011).
20. B. le Feber, J. Cesario, H. Zeijlemaker, N. Rotenberg, and L. Kuipers, "Exploiting long-ranged order in quasiperiodic structures for broadband plasmonic excitation," *Appl. Phys. Lett.* **98**, 201108 (2011).
21. N. Rotenberg, M. Betz, and H. M. van Driel, "Ultrafast all-optical coupling of light to surface plasmon polaritons on plain metal surfaces," *Phys. Rev. Lett.* **105**, 017402 (2010).
22. J. Renger, R. Quidant, N. van Hulst, S. Palomba, and L. Novotny, "Free-space excitation of propagating surface plasmon polaritons by nonlinear four-wave mixing," *Phys. Rev. Lett.* **103**, 266802 (2009).
23. C. Ruppert, J. Neumann, J. B. Kinzel, H. J. Krenner, A. Wixforth, and M. Betz, "Surface acoustic wave mediated coupling of free-space radiation into surface plasmon polaritons on plain metal films," *Phys. Rev. B* **82**, 081416(R) (2010).
24. T. Utikal, M. I. Stockman, A. P. Heberle, M. Lippitz, and H. Giessen, "All-optical control of the ultrafast dynamics of a hybrid plasmonic system," *Phys. Rev. Lett.* **104**, 113903 (2010).

1. Introduction

Interference phenomena are central throughout optical physics and can lead to exciting effects such as quantum coherent control [1], electromagnetically induced transmission [2], time-reversed lasing [3], and the rich behavior of Fano-resonances [4]. In these roles interference can be used in a variety of nanophotonic applications. A textbook example of the applications of interference is the well known diffraction of light from periodic structures, a paradigmatic illustration of the wave nature of light [5]. Surprisingly, the full significance of interference on grating-mediated coupling has so far not been realized. In resonant coupling, gratings provide the momentum necessary to couple light to guided modes such as those of dielectric waveguides [6] or to surface plasmon polaritons (SPPs) [7]. That is, gratings can be used to match the wavevectors of different modes, providing a channel which couples the different modes. Consequently, traditional design of grating couplers focuses on their periodicity and amplitude, ensuring that resonant coupling can occur and maximizing the transfer of energy. Consequently, in describing the resulting flow of energy that can occur the role of the phase of the coupling process is typically neglected, and only the amplitude of the resultant field is considered.

In this work we demonstrate the degree of control that is achievable over a resonant coupling process simply by tuning the geometry of the coupler and thereby the phase of the coupling. Using a plasmonic system as an example, we show that control over just two coupling channels connecting free-space and SPP modes is sufficient to tune the absorption of energy into the plasmonic channel over 6 orders of magnitude, as numerically calculated using rigorous electromagnetic theory. That is, we show that just by changing the relative phase between the two components we can design a coupler that selectively excites SPPs from light that is either incident with a positive or a negative angle, but not both.

We start, in Sec. 2, by considering plasmonic coupling in single component gratings and in particular look for a signature of the role that phase may play in this coupling. In Sec. 3 we turn to double component gratings, where two coupling pathways are simultaneously available, and discuss the consequences of varying the relative phase between these two channels. We place this work within the current framework, highlighting the new aspects with respect to the literature, in Sec. 4, and we then conclude with a brief outlook in Sec. 5.

2. Single component coupling

We begin by considering the grating-mediated resonant energy transfer from an initial mode, with a wavevector component k_i parallel to the surface, to a final mode, associated with k_f , that occurs when an integer multiple of the grating wavevector, G , spans their difference,

$$k_f = k_i + mG, \quad (1)$$

where m is an integer and $G = 2\pi/\Lambda$ for a grating with period Λ . We sketch out this process in Fig. 1(a), showing two pathways for the coupling: for the top pathway two G transitions are required to couple to the guided mode [$m = 2$ in Eq. (1)], while for the bottom pathway only one $2G$ transition is needed ($m = 1$). Physically, the difference between the two cases would be the period of the grating, which would have to double for the situation shown on top, relative to the bottom. We explicitly note that if either, or both, of k_i and k_f represent a guided mode such as a SPP then the coupling is resonant; in this case, even for an arbitrary grating profile, only the component that fulfills Eq. (1) with the smallest possible m need be considered to accurately model the coupling, even for relatively large amplitude gratings with coupling efficiencies in excess of 80% [8]. This is in contrast to non-resonant phenomena such as grating diffraction, where many scattering amplitudes can be of the same magnitude, and hence must all be included in calculations [9–12].

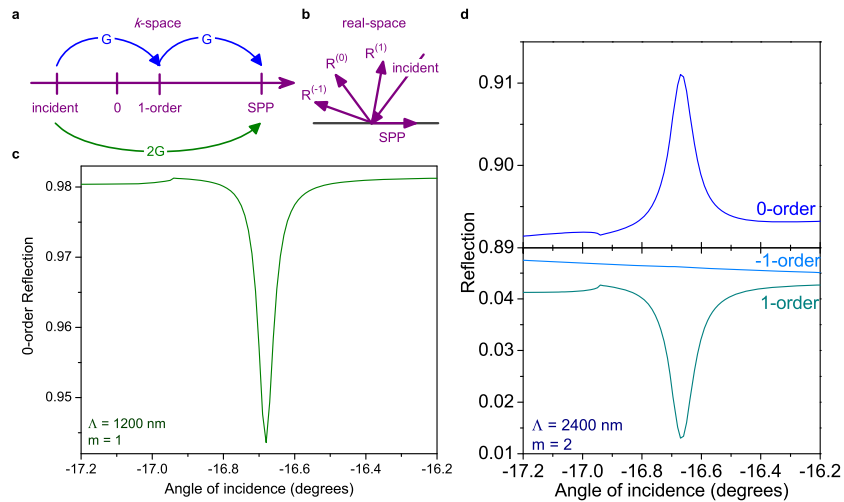


Fig. 1. Grating mediated resonant coupling. A schematic of the process in (a) k -space and (b) real-space, showing the coupling between free-space radiation and a SPP mode. (c) The specular reflection as a function of angle of incidence for the lower pathway shown in (a), showing first order plasmonic coupling (sharp dip) near -16.7 degrees. (d) The different reflected orders as functions of the angle of incidence for the longer period grating (upper pathway from (a)), which show second order plasmonic coupling at the same angle of incidence.

To illustrate the consequences of having two coupling pathways we chose the simplest possible test system, an air-gold interface with a sinusoidal gold grating, where the guided mode is a SPP with the wavevector $k_{sp} = k_0 \sqrt{\epsilon_m / (\epsilon_m + 1)}$ [7]. Here, $k_0 = 2\pi/\lambda$ is the wavevector of light in a vacuum and ϵ_m is the complex dielectric function of gold. We first consider the case where only one coupling pathway is available, where $\lambda = 1500$ nm and $\Lambda = 1200$ nm or 2400 nm, corresponding to the lower and upper pathways of Fig. 1(a), respectively. Note that

when $\Lambda = 2400$ nm we expect several diffracted orders, as well as the SPP to result from the grating diffraction as depicted in Fig. 1(b).

We calculate the reflectivities, $R^{(n)}$ associated with the different reflected orders, using a coordinate transformation method [9, 10] and show the results in Figs. 1(c) and (d). The plasmonic feature is clearly visible in both the specular reflection [$R^{(0)}$, (c) and top panel of (d)] and in the 1-order diffraction [$R^{(1)}$, bottom of (d)] but, surprisingly, it appears in a different manner the different reflectivities. In the example of the shorter period grating ($\Lambda = 1200$ nm) where there are no diffracted orders, energy that would otherwise reflect is coupled to SPPs, and we observe a dip in the reflectivity for angles near -16.7 degrees. A similar transfer of energy to SPPs occurs for the longer period grating ($\Lambda = 2400$ nm), where a dip in $R^{(1)}$ indicates that energy that would otherwise be diffracted is coupled into the SPP. But for the longer period grating the specular reflection is enhanced by the presence of the SPP, as energy flows from the SPP to this order and we observe a peak in $R^{(0)}$. This suggests that in the example of the longer period grating we can view both the dip in $R^{(1)}$ and the peak in $R^{(0)}$ as a flow of energy between the SPP and the reflected orders, but with a different phase, such that the interference is constructive for $R^{(0)}$ and destructive for $R^{(1)}$.

We understand the phase relations exhibited by the spectra shown in Fig. 1(d) by considering the situation depicted in Fig. 1(a). We can write any arbitrary periodic grating profile $h(y)$ as

$$h(y) = \sum_p h_{pG} e^{ipGy}, \quad (2)$$

and hence, in k -space, the amplitude of a grating component with wavevector pG will be represented by Fourier coefficients which we write as $h_{\pm pG}$. To ‘see’ the plasmonic field, the diffracted field must first excite the plasmonic field through interactions with the grating in a $+G$ transition, and then ‘return’ through a $-G$ transition. And, as we have previously shown, the effect of the SPP on the diffracted order will be proportional to $h_G h_{-G}$, which results in a π phase shift [8]. Similarly, the specularly reflected field must gain, and then lose, $2G$ and hence the effect will be proportional to $h_G^2 h_{-G}^2$ and hence results in a 2π phase shift.

Likewise, it is important to consider the SPP field that is excited due to the presence of the grating, when either of the two pathways shown in Fig. 1(a) are available. For the 2400 nm grating the plasmonic coupling amplitude can be written as $\Gamma_{\pm}^{(G)} = ch_{\pm G} h_{\pm G}$, where c is a constant that depends on the geometry and material properties of the system, and likewise for the 1200 nm grating the coupling amplitude is $\Gamma_{\pm}^{(2G)} = c' h_{\pm 2G}$ [8]. However, in these cases the transfer of *energy* to the SPP is proportional to $|\Gamma_{\pm}^{(pG)}|$, where the $+$ is for the situation depicted in the figure, and the $-$ is for its mirror image. That is, such resonant coupling is inherently left-right symmetric and shifting the grating with respect to the incident beam has no effect on the amplitude of the excited SPP.

3. Double harmonic gratings

The signature of interference in the reflectivities suggests that we look for a situation where we can exploit the phase degree-of-freedom to control the resonant coupling; we do this by considering a two component grating where we can control the *relative* phase between the components. Consequently, we turn to the double harmonic grating with the profile

$$h(y) = \frac{a_G}{2} \cos(Gy + \varphi_G) + \frac{a_{2G}}{2} \cos(2Gy + \varphi_{2G}), \quad (3)$$

where the amplitudes a_G and a_{2G} are related to the Fourier harmonics $h_{\pm G}$ and $h_{\pm 2G}$, respectively, and $\varphi_{G,2G}$ are the spatial phases of the two harmonics, which in turn control the phases

of the plasmonic coupling coefficients $\Gamma^{(G,2G)}$. Hence, and in analogy with quantum coherent control experiments [1], we expect the *relative phase parameter*

$$\varphi = \varphi_{2G} - 2\varphi_G, \quad (4)$$

to control the overall plasmonic coupling. In what follows, we set $\varphi_G = 0$ and so $\varphi = \varphi_{2G}$.

Figure 2(a) shows the reflection spectra of the different diffracted orders for a grating with parameters $a_G = 90$ nm, $a_{2G} = 5$ nm, and $\varphi = 0$ degrees, where the amplitudes have been carefully selected to match the coupling strength of the components. In this case, both transitions from the incident radiation to the SPP shown in Fig. 1(a) are available simultaneously. We emphasize that the two coupling channels – the G and the $2G$ pathways – excite the same

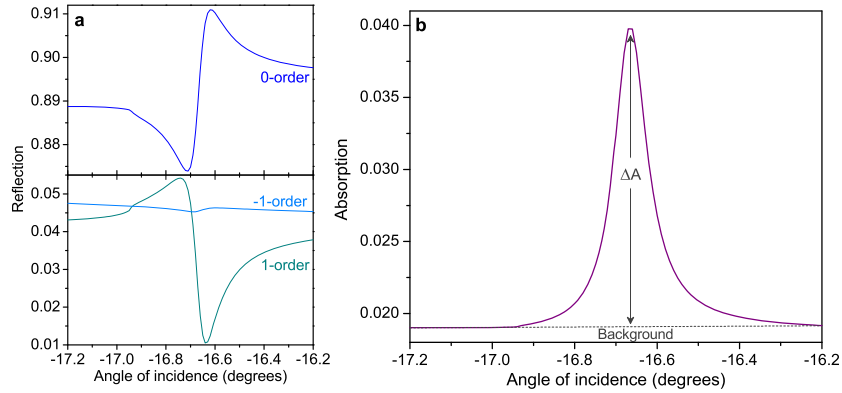


Fig. 2. Double harmonic plasmonic coupling. (a) Reflection spectra for the different diffracted orders of a double harmonic grating. (b) The corresponding absorption spectrum for this grating, exhibiting a clear plasmonic absorption resonance near -16.7 degrees. The peak absorption into the plasmonic mode, ΔA , is shown with respect to the ambient background absorption of the grating (horizontal dashed line).

plasmonic mode, albeit with different phases, and hence we expect that they interfere. Indeed, we observe a dispersive line-shape in the reflectivity, which is reminiscent of a Fano resonance, and which clearly demonstrates that the phases of the excited SPPs play an important role in the overall plasmonic coupling. The source of the interference is particularly obvious if we again consider the energy flow into the SPP. When the two pathways are available, then the coupling is proportional to $|\Gamma_{\pm}^{(G)} + \Gamma_{\pm}^{(2G)}|^2$, which contains the interference term $\Gamma_{\pm}^{(G)}\Gamma_{\pm}^{(2G)*} + c.c.$

The complex shape of the reflectivities brought about by the interference in the plasmonic coupling make it difficult to identify how much energy couples to the SPP, and consequently we look at the absorption of the grating coupler,

$$A = 1 - \sum_n R^{(n)}, \quad (5)$$

where n denotes the different diffracted orders. In this manner, the absorption includes both the direct ohmic losses as well as the energy which is first coupled into the SPPs and therefore does not re-radiate into free-space. Figure 2(b) shows this absorption and allows for the clear separation of the two mechanisms: the direct ohmic losses appear as a relatively flat ambient value of ~ 0.019 , while the plasmonic coupling appears as a sharp spectral bump near -16.7 degrees which peaks at a value ~ 0.040 . The difference between the two values, ΔA , represents the portion of energy which couples to the SPPs. While the interference between the coupling

channels can manifest as either an amplitude increase or decrease of the different diffracted modes, the net absorption is always increased due to the plasmonic coupling.

The most dramatic effect that we observe is the degree to which the plasmonic coupling can be controlled by simply tuning φ , as shown in Fig. 3. Even with this simple geometry, it is possible to suppress the energy that flows into SPPs by a factor of over 10^6 . For example, for

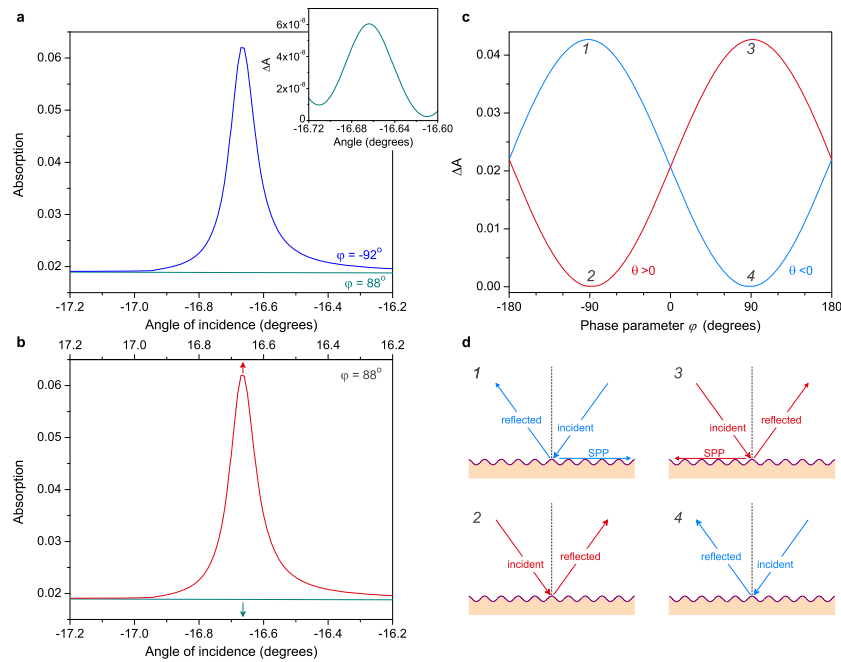


Fig. 3. Phase dependent resonant coupling. (a) Absorption spectra for negative incidence angles for the cases of maximum ($\varphi = -92^\circ$) and minimum ($\varphi = 88^\circ$) coupling, corresponding to points 1 and 4 in part (c). The inset shows that, in the region near the angle of optimal plasmonic coupling, for $\varphi = 88^\circ$, only 5×10^{-8} of the energy couples to the SPP mode. (b) The absorption spectra for both positive and negative angles of incidence for $\varphi = 88^\circ$, corresponding to points 3 and 4 in part (c), showing that only light that is incident with positive angles couples to SPPs. (c) The energy absorbed into the plasmonic mode as a function of the relative phase of the grating components. (d) Schematic representations of points 1-4 of (c), where points 1 and 4 corresponds to the situation shown in Fig. 1(a). All situations include diffracted beams which are omitted for clarity.

negative angles of incidence near -16.7 degrees [Fig. 3(a)], when the $2G$ grating component lags behind that of the G grating by almost a quarter period, we find that the SPPs coupled by the two grating components are in phase and ΔA peaks above 0.04. Conversely, it is possible to minimize ΔA to 5×10^{-8} when the $2G$ component leads by a quarter period and destructive interference quenches the plasmonic coupling. Remarkably, the suppression of the coupling occurs for all angles of incidence, peaking at values of $\Delta A < 6 \times 10^{-8}$ as shown in the inset of this figure.

We now investigate the left-right coupling symmetry of our grating structure by fixing φ at 88° and determining the absorption spectrum for both positive and negative angles of incidence. As Fig. 3(b) shows, for this relative phase light that is incident at +16.7 degrees is maximally coupled to SPPs, while almost no coupling occurs for light incident from the negative direction. In essence, we break the coupling symmetry of this structure merely by properly setting the

relative phase of the two grating components: when light is incident from the positive direction the coupling G and $2G$ coupling channels constructively interfere, while for negative incidence the two channels interfere destructively and no coupling occurs. This symmetry breaking is shown in Fig. 3(c), where we map the phase-dependence of ΔA . As expected the structure, and hence the coupling, is symmetric for $\varphi = 0, \pm 180$ degrees. The extreme cases, denoted by 1 through 4, are shown schematically in Fig. 3(d), and are found near $\varphi = \pm 90$ degrees; here we explicitly show when plasmonic coupling occurs (1, 3, dark state) and when it does not (2, 4, perfect-diffractor), appearing as a sort of plasmonic diode. We attribute the 2 degree offsets with respect to ± 90 degrees to the inclusion of higher-order coupling processes in our calculations.

At a first glance, this sort of directional coupling might appear to violate reciprocity, which essentially states that in a linear system one should be able to swap the source and the detector and obtain the same optical response. Consider, for example, situations 3 and 4 of Fig. 3(d), whose corresponding absorption spectra are shown in part (b) of this figure. Their absorption spectra differ greatly, due to SPP excitation for light incidence from the left and not from the right. Thus one might naively expect that the coefficients of reflection in the two situations would also differ greatly and, since the two situations correspond to a swap of source and detector, that this would violate reciprocity.

The calculations presented in Fig. 4 show that reciprocity is actually not violated, as expected for our time independent, linear system [13]. Despite the fact that the coupling into the SPP is roughly a million times stronger for positive incident angles (case 3) than for negative angles (case 4), the specular reflection spectra of the two cases are identical, respecting reciprocity. The ‘missing’ energy can be located in the diffracted orders. In Fig. 4(b), which shows the

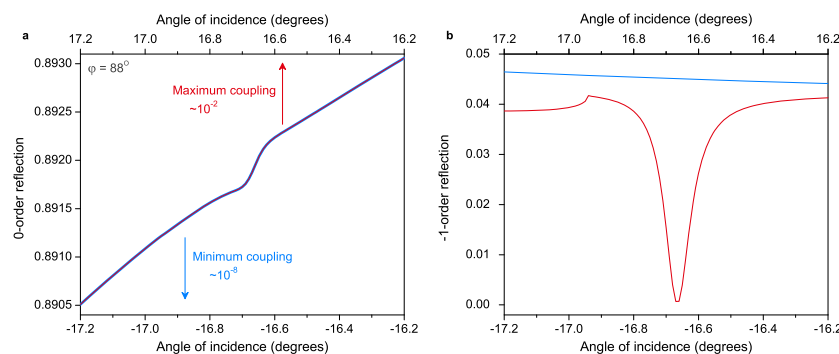


Fig. 4. The (a) 0- and (b) -1-order reflection spectra for both positive and negative incidence when the relative phase of the grating components is 88 degrees, corresponding to cases 3 and 4 of Fig. 3(c) and (d). Although the plasmonic coupling of the two cases differ by 6 orders of magnitude, their 0-order spectra are identical while only the -1-order spectra for positive incidence shows a significant plasmonic feature.

1-order reflection, we observe a plasmonic feature for incidence near 16.7 degrees but not near -16.7 degrees. Remarkably, the interference in the coupling processes essentially acts to suppress energy transfer from the specular reflection to the SPP, while maximizing that from the diffracted orders. Not only is it possible to tune the magnitude of the plasmonic coupling using the relative phase (φ) of the two grating components, but varying this parameter also allows us to change which of the diffracted orders provides the energy for the SPP.

Finally, we briefly turn to the importance of the height parameters, a_G and a_{2G} , of Eq. (3). Generally, increasing the amplitude of a grating component leads to a corresponding increase of the plasmonic coupling. Consequently, if we wish to effectively interfere the different coupling channels, an increase or decrease of one component must be accounted for with a similar

change of the other component. However, since the $2G$ channel is a first-order coupling mechanism, while the G coupling is a second-order event, there is no linear correspondence to the relative changes of the components. Figure 5 shows the phase-dependent plasmonic absorption for different grating heights. As expected, by increasing the a_{2G} amplitude and suitably

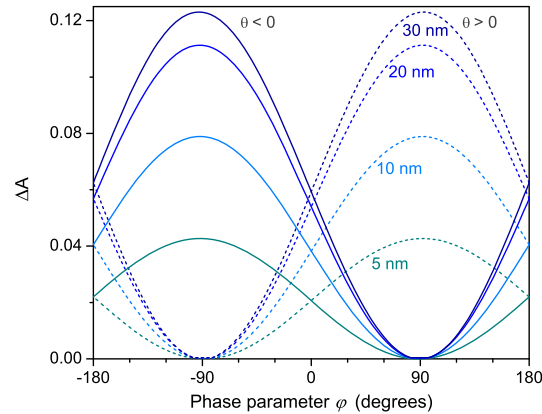


Fig. 5. Dependence of the plasmonic absorption on the grating amplitudes. ΔA as a function of phase for both positive and negative angles of incidence for $a_{2G} = 5, 10, 20$ and 30 nm. The corresponding a_G amplitudes are $90, 126, 174,$ and 208 nm.

matching a_G we are able to fix the minimum coupling near zero while increasing the maximal coupling. In fact, by increasing a_{2G} from 5 to 30 nm (and a_G from 90 to 208 nm) we triple the plasmonic coupling, from 0.042 to 0.12 . However, as this figure shows, the achievable gain in plasmonic coupling saturates with increasing amplitudes. This is perhaps unexpected since single component gratings can couple in excess of 0.9 of the energy to plasmonic modes. However, we note that at the peak, the energy couples from the diffracted modes to the SPP and hence the effectiveness of this coupler is limited by its diffraction efficiency. Further, we hypothesize that for the large grating amplitudes, and in particular for a large a_G component, higher order processes can no longer be neglected. That is, with these large amplitudes it might not be possible to optimize both the minimum and maximum achievable coupling with only two grating components, and third or fourth grating harmonics might be required.

4. Historical context

In order to highlight the new concepts in our work, we now attempt to place it within the context of previous literature pertaining to grating diffraction in general, and to plasmonic coupling in particular. This section is by no means a comprehensive review of this subject, and is rather meant to highlight the new concept introduced in this work.

Our proposed structure might seem simply to constitute the plasmonic equivalent of a blazed grating, where an asymmetric profile such as a tilted sinusoid or triangle is used to optimize diffraction into a specific free-space order [14]. But while there are similarities between our approach to plasmonic coupling and blazed diffraction gratings – in both cases there are multiple grating harmonics with an interplay that determines the coupling or diffraction efficiencies – there are fundamental differences.

First, in our scenario we consider a resonant coupling process, and as such only the first few grating harmonics are needed and, more importantly, only the propagating fields (in our case, the incident, diffracted, and SPP) are considered [8]. In contrast, for blazed gratings, the non-resonant diffraction into free-space modes necessitates the inclusion of fields at many

(often hundreds of) wavevectors to accurately describe the interaction between the light and the grating [9, 11].

More importantly, our protocol differs in a fundamental way from the practice of blazed gratings in its use of the different grating harmonics. In our approach, the amplitudes of the two harmonics have been carefully matched so that, individually, they couple the same amount of energy to the SPPs. Consequently, the height of the G component is much larger than that of the $2G$ component, for example in the cases shown in Figs. 2 and 3 $a_G = 90$ nm and $a_{2G} = 5$ nm. Hence, in our case we have two coupling pathways of equal amplitude interfering, which affords us the extreme degree of control over the plasmonic coupling that has been demonstrated above. In contrast, for blazed diffraction gratings, where there is no resonant coupling, the amplitudes of the first couple higher harmonics tend to be comparable to the fundamental component. Here, the higher grating harmonics fine-tune the diffraction. Alternatively, a very asymmetric profile can be used to, for example, maximize the h_{-G} Fourier component with respect to the h_G component and in doing so diffract, or even couple [15] preferentially in one direction. However, in this case the phases of the different components do not play a significant role as they do not interfere.

Finally, there have been many studies on the influence of the grating profile on plasmonic coupling, of which the works of Sambles and co-workers [16, 17] are excellent examples. There, as in our work, the grating profile is broken into its harmonics and equations reminiscent of Eqs. (2) or (3) can be found. In fact, in many of these works the fundamental (G) grating component couples directly to the SPP and hence the higher grating harmonics ($2G$, $3G$, etc.), which have smaller amplitudes, are the ones that provide higher order coupling pathways. Again, as with the blazed gratings, the higher harmonics provide a way to *fine-tune* the plasmonic coupling, in contrast to our work where the coupling pathways of the two harmonics interfere with equal amplitudes. In essence, we introduce the concept of using the phase between the grating components to completely change the way a grating couples light to SPPs, rather than just controlling the fine details.

We note that bi-periodic gratings have appeared in other branches of the literature, for example as an element of a distributed feedback laser where the introduction of the second grating component was shown to reduce radiative losses [18]. However, in this case the amplitudes of both components are equal, and only one of the component resonantly couples to laser modes to free-space radiation. The second grating component introduces a Bragg reflector to the structure, which opens up a photonic bandgap [16] and hence reduces the radiative losses. Again, this is fundamentally different than our approach where the two grating components offer coupling pathways which interfere.

5. Conclusion and outlook

To conclude, we have demonstrated that unprecedented control of plasmonic coupling is possible by exploiting a previously neglected degree-of-freedom, the relative phase parameter of different grating components, which allows for the interference of different coupling channels. This is in stark contrast to previous advances in plasmonic coupling, where gratings are cleverly designed with profiles that are highly asymmetric [15] or quasi-periodic [19, 20] in order to control single component plasmonic coupling. Even in instances where many such channels are present, they operate independently from each other; for example, the different components of a quasi-periodic array may simultaneously couple light of different frequencies to SPPs. In our work what allows us to achieve coupling contrasts of over 10^6 is the interference between the different channels. In principle, our design is only limited by the diffraction efficiency of the grating structure, which routinely approaches 0.8 in commercial gratings. This suggests that with optimization, grating couplers based on our paradigm could essentially act like pho-

tonic diodes, where energy is only coupled to a specific channel for one direction of incidence. Further, although for our demonstration we used a single bi-harmonic grating, similar control over the plasmonic coupling should be achievable using more easily fabricated structures such as one where the grating harmonics are layered. This control could be made even more powerful if one could actively control the phase of one of the grating components, perhaps in a linear [21] or nonlinear [22] all-optical manner, or electrically [18,23]. Another powerful alternative would be to combine our approach with all-optical coherent control in hybrid plasmonic systems, where the structure is passive but an additional control pulse is introduced [24]. In these cases it should be possible to both choose the directionality as well as tune the magnitude of the coupling on ultrafast time scales.

Although we demonstrated that the coupling of free-space modes to SPPs can be controlled through the interference of two coupling channels with gratings, this interference based approach is much more general. Essentially, one can control the coupling of any two modes in this fashion as long as there is a resonant energy transfer, and hence this approach can be used with any combination of waveguide modes, (long-range) plasmonic modes, and free-space radiation. In this sense, this approach to geometric control of resonant coupling should find use in diverse on-chip applications, from the coupling of light to SPPs as demonstrated herein, to coupling different photonic crystal waveguide modes. Finally, it is worth noting that even though we have demonstrated the potential of this approach to plasmonic coupling, we have in no way tailored our structures for these applications. Rather, our focus has been the introduction of a new photonic tool, and consequently we predict that substantial improvements can be made during the design of any device that relies on our approach.

Acknowledgment

This work is part of the research program of the Stichting voor Fundamenteel Onderzoek der Materie (FOM), which is financially supported by the Nederlandse Organisatie voor Wetenschappelijk Onderzoek (NWO). This work is supported by NanoNextNL of the Dutch ministry EL&I and 130 partners, and by the EU FET project “SPANGL4Q”. JES acknowledges financial support from the Natural Sciences and Engineering Research Council of Canada (NSERC).